mally exposed to laboratory light, no significant differences were noted in the absorption spectra (460–900 nm) as a function of time.

The resonance Raman spectrum using 457.9-nm excitation (900–1650 cm^{-1}), in air, of the ZnTPP adsorbed onto PVG (Figure 3B) is quite distinct from the spectrum of solid ZnTPP (Figure 3C) or the previously reported[4] spectra of the cation radical in solution. In the spectral region above 900 cm^{-1}, a band at 1596 cm^{-1} is most prominent in the PVG-adsorbed sample, whereas solid ZnTPP shows several equally prominent bands at 1552, 1359, and 1238 cm^{-1}. The previously reported resonance Raman spectrum of the ZnTPP cation radical is not unlike that of ZnTPP, showing only small frequency shifts from the ZnTPP spectrum. The resonance-enhanced Raman spectrum of the isoporphyrin generated by ceric oxidation of an ethanolic solution of ZnTPP (Figure 3A) shows a strong band at 1588 cm^{-1} in the high-frequency spectral region. There is no evidence of the strong 1552-cm^{-1} ZnTPP band in the PVG adsorbate spectrum. The same is true of the 1359-cm^{-1} band. The broad features in the PVG adsorbate spectrum (Figure 3B) at 1424 and 1328 cm^{-1} may correspond to isoporphyrin bands at 1415 and 1340 cm^{-1}, respectively, in Figure 3A. The broadness of these Raman features for the PVG adsorbate spectrum is attributable to the heterogeneity of the reaction products being sampled (see discussion of the absorption spectrum above). An additional contribution to heterogeneity is likely due to the fact that various surface silanol groups and/or surface-bonded water molecules are the nucleophiles active in forming isoporphyrin. The Raman band at 1596 cm^{-1} is reasonably assigned as the analogue to the 1552-cm^{-1} ZnTPP band, upshifted by 44 cm^{-1} due to the reduction in the π-conjugation path for the methine-reduced isoporphyrin species. This is also reflected in the large changes seen in the visible spectra. The 457.9-nm resonance excitation favors the selection of Raman scattering from the isoporphyrin species on the glass because of the associated 440-nm Soret band. Resonance Raman spectroscopy using excitation to the red of 457.9 nm is prohibited by strong luminescence, which swamps the Raman signals. The possible photodegradation of adsorbed metalloporphyrin was minimized by defocusing the laser excitation source. Rescanning of key spectral regions to assure constant scattering levels was used to monitor for photodegradation.

Although not anticipated, the oxidation of an adsorbate by PVG is not unique. A previous report[5] details the oxidation of 1,1-diphenylethylene (DPE) upon adsorption onto PVG. This oxidation also produced a cation radical species, which was stabilized and detected spectroscopically. The DPE oxidation was attributed to Lewis acid sites on the PVG surface. The oxidation of ZnTPP and TPP reported here indicates that such sites may act as oxidizers for a wider variety of molecules.

In contrast to our findings, Raman studies[6] of NiTPP adsorbed onto more conventional supports such as silica and alumina fail to show any adsorption-induced changes. Furthermore, heating NiTPP adsorbed on silica at 300 °C in nitrogen produced no spectral changes before the onset of decomposition. Similar experiments on alumina produced only relative intensity changes in the Raman bands before decomposition set in.

In summary, the resonance Raman and absorption spectra establish the presence of isoporphyrin species on the PVG surface after adsorption of ZnTPP. Previous studies have shown that these arise via nucleophilic attack on the dication produced by oxidation of the ZnTPP. On the PVG surface, adsorbed water and/or silanol groups would be the likely nucleophiles. The formation of oxidized ZnTPP is evidenced by the EPR spectra of the π cation radical form for both ZnTPP and TPP. The dication is not directly observed in any of our experiments, but its presence is inferred from the isoporphyrin substitution product. Further, the nature of the oxygen dependence of the EPR signal indicates that some type of oxygen adduct of the radical may be involved in the route leading to isoporphyrin formation. No significant reaction occurs if ZnTPP is adsorbed in the absence of oxygen.

Experiments with several other metallotetraphenylporphyrins, including Fe^{III}(TPP)Cl, CuTPP and Ru(CO)TPP indicate that these oxidations are a general phenomenon associated with adsorption onto the PVG surface. Further characterization of these reactions is continuing in our laboratory.

Experimental Section

ZnTPP and TPP were purchased from Man-Win Chemical Co. and subjected to chromatography on alumina before use. All solvents were spectroquality grade. Samples were adsorbed onto pretreated PVG as previously described.[7,8] For Raman and optical absorption measurements, pieces of PVG about 25 mm × 25 mm × 4 mm were used. For EPR experiments, the PVG was crushed into pieces small enough to fit a 3-mm-i.d. quartz EPR tube, before adsorption experiments.

Absorption spectra were recorded on a Cary 14 or a Perkin-Elmer Lambda 3 UV–visible spectrophotometer. Electron Paramagnetic Resonance spectra were recorded on an IBM Instruments ER200E-SCR EPR machine (9-in. magnet). Resonance Raman spectra were recorded by using a previously described system.[9]

Acknowledgment. Support for this research by the City University of New York research awards program and the Dow Chemical Co. Technology Acquisition Program is gratefully acknowledged. We would also like to thank Professor Thomas G. Spiro of Princeton University for helpful discussions.

Registry No. ZnTPP, 14074-80-7; $ZnTPP^{+\cdot}$, 39732-73-5; TPP, 917-23-7; $TPP^{+\cdot}$, 34479-64-6.

(4) Yamaguchi, H.; Nakano, M.; Itoh, K. *Chem. Lett.* **1982**, 1397.
(5) Yamamoto, Y.; Yamada, H. *J. Raman Spectrosc.* **1982**, *12*, 157.
(6) Streusand, G. B. J.; Schrader, G. L. *Appl. Spectrosc.* **1984**, *38*, 433.
(7) Simon, R.; Gafney, H. D.; Morse, D. L. *Inorg. Chem.* **1983**, *22*, 573.
(8) Basu, A.; Gafney, H. D.; Perettie, D. J.; Clark, J. B. *J. Phys. Chem.* **1983**, *87*, 4532.
(9) Valance, W. G.; Strekas, T. C. *J. Phys. Chem.* **1982**, *86*, 1804.

Contribution from the Department of Chemistry,
University of New Mexico,
Albuquerque, New Mexico 87131

Preparation and Structure of a Neodymium Complex Containing Bidentate (Carbamoylmethyl)phosphine Oxide Ligands

L. J. Caudle, E. N. Duesler, and R. T. Paine*

Received April 25, 1985

Several groups have studied the metal ion extraction chemistry of bis(phosphine oxides).[1-3] Contrary to expectations it has been observed that with ligands of the type $R_2P(O)CH_2P(O)R_2$ replacement of alkyl groups, R, with phenyl groups, Ph, results in enhanced extraction ability at high acid concentrations for the phenyl-substituted bifunctional ligands. The so-called "aryl strengthening effect" has been rationalized in terms of an entropic stabilization in the extraction process;[1] however, a thorough understanding of the coordination chemistry of these ligands at the molecular level has not been obtained. In similar systems, Horwitz and co-workers[4] have found that replacement of alkoxy groups on (carbamoylmethyl)phosphonates (CMP's), $(RO)_2P(O)CH_2C(O)NR_2'$, with alkyl groups leads to larger liquid–liquid extraction coefficients ($K_D = [M_{org}]/[M_{aq}]$) for actinide ions.

(1) Lobana, T. S.; Sandhu, S. S. *Coord. Chem. Rev.* **1982**, *47*, 282 and references therein.
(2) Myasoedov, B. F.; Chmutova, M. K.; Karalov, Z. K. In "Actinide Separations"; American Chemical Society: Washington, DC, 1980; ACS Symp. Ser. No. 117, p 101 and references therein.
(3) Rozen, A. M.; Nikolotova, Z. I.; Kartasheva, N. A.; Skotnikov, A. S. *Radiokhimiya* **1983**, *25*, 603.
(4) Horwitz, E. P.; Kalina, D. G.; Kaplan, K.; Mason, G. W.; Diamond, H. *Sep. Sci. Technol.* **1982**, *17*, 1261.

0020-1669/85/1324-4441$01.50/0

Table I. Crystallographic Data for $Nd(NO_3)_3[Ph_2P(O)CH_2C(O)NEt_2]_2 \cdot 2MeCN$

(A) Crystal Parameters at 21 °C	
cryst syst	monoclinic
space group	$P2_1/c$
a, Å	17.273 (9)
b, Å	16.837 (8)
c, Å	18.219 (9)
β, deg	117.11 (2)
Z	4
V, Å^3	4716.4 (4)
M_r	1043.06
ρ_{calcd}, g cm^{-3}	1.47
μ(Mo Kα), cm^{-1}	12.4
F(000)	2132.

(B) Data Collection	
diffractometer	Syntex P3/F
radiation	Mo Kα (λ = 0.71069 Å)
monochromator	highly oriented graphite cryst
reflcns measd	$\pm h, +k, \pm l$
2θ range, deg	1 - 55
scan type	$\theta - 2\theta$
scan speed (in 2θ), deg min^{-1}	6-30
scan range, deg	from $2\theta(K\alpha_1)$ - 1.1 to $2\theta(K\alpha_1)$ + 1.1
bkgd measd	stationary cryst and counter; at the beginning and end of each 2θ scan each for half the total 2θ scan time
std reflcns	3 reflcns every 141 refcns; [$\bar{5}00$, $0\bar{8}0$, $00\bar{4}$]
no. of unique reflcns collcd	9765
no. of obsd reflcns used in refinement	6511 with $F > 4\sigma(F)$
weighting scheme	$1/[\sigma(F)^2]$
no. of params	553

They have also reported that a mixed phenyl–alkyl-substituted ligand. (Ph)(*n*-octyl)$P(O)CH_2C(O)N(i\text{-}Bu)_2$, is a particularly powerful actinide extractant. During the course of these studies we have examined several coordination complexes formed by CMP ligands with lanthanide and actinide ions.[5-8] Our studies have been helpful in guiding subsequent architectural modifications on the CMP extractant backbone and in testing models for new extraction systems. In this regard we were interested in determining if a structural basis for the aryl strengthening effect might be found in properly substituted CMP ligands. We have recently reported the synthesis of the (carbamoylmethyl)phosphine oxide $Ph_2P(O)CH_2C(O)NEt_2$ (**1**)[9] and its coordination chemistry with UO_2^{2+}. We report here the formation of a complex $Nd(NO_3)_3[Ph_2P(O)CH_2C(O)NEt_2]_2$ (**2**), the molecular structure determination for the solvated complex $Nd(NO_3)_3[Ph_2P(O)CH_2C(O)NEt_2]_2 \cdot 2MeCN$ (**3**), and a comparison of the structure of this complex with the structure of a related CMP–lanthanide complex, $Sm(NO_3)_3[(i\text{-}PrO)_2P(O)CH_2C(O)NEt_2]_2$ (**4**).

Experimental Section

Preparation. Complex **2** was prepared by the addition of 12 mmol of $Nd(NO_3)_3 \cdot 6H_2O$ in warm ethanol to 24 mmol of $Ph_2P(O)CH_2C(O)NEt_2$ in warm ethanol. The combination was stirred and allowed to evaporate slowly in air over several days. The resulting pale lilac-colored powdery solid was washed with cold ethanol and air-dried. Anal. Calcd for $NdP_2O_{13}N_5C_{36}H_{44}$: C, 45.00; H, 4.62; N, 7.29. Found: C, 45.27; H, 4.90; N, 7.16. Infrared spectrum (cm^{-1}, KBr pellet) 3060 m, 2970 m, 2939 m, 1590 s, 1450 s, br, 1383 w, 1310 s, 1295 s, 1220 w, 1150 s, 1122 m, 1096 m, 1070 w, 1035 m, 995 w, 955 m. The complex is soluble in boiling water, MeOH, EtOH, $CHCl_3$, and CH_3CN.[10] A crystal suitable for single-crystal X-ray diffraction analysis was obtained by very slow cooling of a hot, saturated CH_3CN solution of the complex.

X-ray Crystallography. A pale lilac-colored single crystal, 0.12 mm × 0.46 mm × 0.62 mm, was mounted in a glass capillary along with a small amount of mother liquor. The crystal was centered on a P3/F automated diffractometer, and the determinations of the crystal class, orientation matrix, and unit cell dimensions were performed in a standard manner.[11] Data were collected in the θ–2θ mode with use of Mo Kα radiation, a scintillation counter, and a pulse-height analyzer. A summary of data collection parameters appears in Table I. Inspection of the data revealed systematic absences $l = 2n + 1$ for $h0l$ and $k = 2n + 1$ for $0k0$, and the monoclinic space group $P2_1/c$ was indicated. A small empirical absorption correction based on Ψ scans was applied to the data; the agreement factor on 288 Ψ scans (8 reflections measured 36 times) was 5.8% before and 5.7% after the absorption correction. The estimated minimum and maximum transmission factors were 0.997 and 0.907. The redundant and equivalent data were averaged and converted to unscaled $|F_o|$ values following corrections for Lorentz and polarization effects.

The Nd atom position was determined from the Patterson map and the remaining non-hydrogen atom positions were located by difference Fourier syntheses.[11,12] Isotropic refinement on the non-hydrogen atoms led to R_F = 11.3%. Anisotropic refinements on all non-hydrogen atoms except the solvent molecules gave R_F = 8.5%. Anisotropic refinement on one of the solvent molecules and addition of the hydrogen atoms in idealized positions led to final least-squares refinements with R_F = 6.35%, R_{wF} = 4.98% and GOF = 1.47. The final difference Fourier synthesis revealed no unusual features. There were two peaks over 1.0 e/Å^3, and both were quite close to the Nd atom. Final positional parameters are given in Table II. Tables of observed and calculated structure factors, anisotropic thermal parameters, and hydrogen atom positional and isotropic thermal parameters are given in the supplementary material along with a complete listing of bond distances and angles.

Results and Discussion

The combination of $Ph_2P(O)CH_2C(O)NEt_2$ (**1**) with $Nd(NO_3)_3$ in a 2:1 ratio in ethanol results in the formation of the powdery solid **2** whose stoichiometry, $Nd(NO_3)_3[Ph_2P(O)CH_2C(O)NEt_2]_2$, is deduced from elemental analyses.[13] The infrared spectrum of **2** (KBr) shows strong absorptions at 1590 and 1150 cm^{-1}, which are assigned to the carbonyl and phosphoryl stretching frequencies, respectively. These absorptions represent coordination shifts of $\Delta\nu_{CO} = -40$ cm^{-1} and $\Delta\nu_{PO} = -55$ cm^{-1} relative to the absorptions of ligand **1**,[9] and these shifts can be compared with those found for $Sm(NO_3)_3[(i\text{-}PrO)_2P(O)CH_2C(O)NEt_2]_2$: $\Delta\nu_{CO} = -56$ cm^{-1} and $\Delta\nu_{PO} = -49$ cm^{-1}. Coordination shifts of this magnitude in lanthanide–CMP complexes have been used previously to indicate bidentate coordination of a CMP ligand, and where this conclusion has been drawn, the bidentate coordination mode has been subsequently confirmed by single-crystal X-ray diffraction structure determinations.[5-8,14] The analytical and infrared data offer no evidence for solvation of **2** obtained in this fashion.

The formula of **2**, $M(NO_3)_3(L)_2$, established from elemental analyses compares with that found in $Sm(NO_3)_3[(i\text{-}PrO)_2P(O)CH_2C(O)NEt_2]_2$ (**4**), and the molecular structure of the latter contains two bidentate CMP ligands.[6] It was, therefore, of interest to determine the molecular structure of **2** in order to assess the denticity displayed by the phosphine oxide ligand **1**, as well as to seek some structural evidence for the "aryl strengthening effect". Suitable single crystals were obtained only by slow cooling of a hot acetonitrile solution of **2**. The crystals, in the absence of mother liquor, revert to a powder. The single-crystal X-ray diffraction analysis shows that the crystals contain monomeric units of **2** with four molecules per unit cell, as well as eight solvent molecules (CH_3CN), which are *not* bonded to Nd(III).[15] A view

(5) Bowen, S. M.; Duesler, E. N.; Paine, R. T. *Inorg. Chem.* **1982**, *21*, 261.
(6) Bowen, S. M.; Duesler, E. N.; Paine, R. T. *Inorg. Chim. Acta* **1982**, *61*, 155.
(7) Bowen, S. M.; Duesler, E. N.; Paine, R. T. *Inorg. Chem.* **1983**, *22*, 286.
(8) Bowen, S. M.; Duesler, E. N.; Paine, R. T.; Campana, C. F. *Inorg. Chim. Acta* **1982**, *59*, 53.
(9) Caudle, L. J.; Duesler, E. N.; Paine, R. T., submitted for publication.
(10) Complex **2** is not sufficiently soluble at 25 °C to obtain useful ^{1}H or ^{31}NMR data.
(11) Sheldrick, G. M. "Nicolet SHELXTL Operations Manual"; Nicolet XRD Corp.: Cupertino, CA, 1981. SHELXTL uses scattering factors compiled in: "International Tables for X-ray Crystallography"; Kynoch Press: Birmingham, England, 1968; Vol. IV.
(12) A general description of the least-squares algebra is found in: Ahmed, F. R., Hall, S. R., Huber, C. P., Eds. "Crystallographic Computing"; Munksgaard Publishing Co. Copenhagen, 1970; p 187.
(13) Complexes $M(NO_3)_3[Ph_2P(O)CH_2C(O)NEt_2]_2$ with M = La, Sm, Eu, and Gd were also prepared and characterized. Elemental analyses are consistent with the stoichiometry $Ln(NO_3)_3(\mathbf{1})_2$, established for **2**. X-ray powder diffraction patterns reveal that these complexes are isostructural.
(14) Bowen, S. M. Ph.D. Thesis, University of New Mexico, Albuquerque, NM, 1983.

Table II. Final Positional Parameters for $Nd(NO_3)_3[Ph_2P(O)CH_2C(O)NEt_2]_2 \cdot 2MeCN$

atom	x/a	y/b	z/c	atom	x/a	y/b	z/c
Nd	0.29625 (2)	0.01175 (2)	0.21257 (2)	C(24)	0.6404 (5)	−0.2338 (5)	0.4588 (5)
P(1)	0.13291 (11)	0.13512 (9)	0.04913 (10)	C(25)	0.3278 (4)	−0.0556 (4)	0.4767 (4)
O(1)	0.2240 (2)	0.1092 (2)	0.1013 (2)	C(26)	0.2582 (5)	−0.0055 (5)	0.4569 (5)
C(1)	0.0576 (4)	0.0893 (3)	0.0804 (3)	C(27)	0.2483 (7)	0.0347 (6)	0.5162 (6)
C(2)	0.0924 (4)	0.0946 (3)	0.1728 (4)	C(28)	0.3104 (7)	0.0278 (5)	0.5978 (6)
O(2)	0.1640 (3)	0.0626 (2)	0.2193 (2)	C(29)	0.3798 (5)	−0.0196 (4)	0.6198 (4)
N(1)	0.0466 (4)	0.1309 (3)	0.2054 (3)	C(30)	0.3903 (4)	−0.0605 (4)	0.5590 (4)
C(3)	0.0853 (5)	0.1350 (5)	0.2967 (4)	C(31)	0.3187 (4)	−0.2110 (3)	0.4031 (4)
C(4)	0.1483 (5)	0.2019 (5)	0.3326 (5)	C(32)	0.3180 (4)	−0.2433 (4)	0.4720 (4)
C(5)	−0.0503 (6)	0.1565 (5)	0.1558 (5)	C(33)	0.3115 (5)	−0.3240 (5)	0.4787 (5)
C(6)	−0.0524 (7)	0.2374 (6)	0.1509 (7)	C(34)	0.3094 (5)	−0.3728 (4)	0.4198 (6)
C(7)	0.1213 (4)	0.2405 (3)	0.0595 (4)	C(35)	0.3088 (7)	−0.3430 (4)	0.3485 (6)
C(8)	0.0585 (5)	0.2864 (4)	−0.0014 (5)	C(36)	0.3129 (5)	−0.2605 (4)	0.3405 (5)
C(9)	0.0491 (5)	0.3653 (4)	0.0170 (5)	N(3)	0.3797 (3)	0.1432 (3)	0.3426 (3)
C(10)	0.0981 (5)	0.3961 (4)	0.0908 (5)	O(5)	0.3285 (3)	0.1604 (2)	0.2707 (3)
C(11)	0.1624 (5)	0.3518 (4)	0.1528 (5)	O(6)	0.3891 (3)	0.0696 (2)	0.3584 (3)
C(12)	0.1738 (5)	0.2732 (4)	0.1361 (4)	O(7)	0.4195 (3)	0.1923 (3)	0.3950 (3)
C(13)	0.0957 (4)	0.1081 (3)	−0.0572 (4)	N(4)	0.1913 (4)	−0.1264 (3)	0.0991 (3)
C(14)	0.1554 (5)	0.0786 (4)	−0.0811 (4)	O(8)	0.2664 (3)	−0.1394 (2)	0.1571 (3)
C(15)	0.1287 (5)	0.0558 (4)	−0.1623 (4)	O(9)	0.1652 (3)	−0.0552 (3)	0.0914 (3)
C(16)	0.0440 (5)	0.0613 (4)	−0.2185 (4)	O(10)	0.1454 (3)	−0.1785 (3)	0.0534 (3)
C(17)	−0.0157 (5)	0.0907 (4)	−0.1960 (4)	N(5)	0.4082 (4)	0.0389 (3)	0.1310 (4)
C(18)	0.0083 (4)	0.1143 (4)	−0.1152 (4)	O(11)	0.3496 (3)	−0.0129 (3)	0.1060 (3)
P(2)	0.33785 (11)	−0.10725 (9)	0.39468 (10)	O(12)	0.4178 (3)	0.0782 (2)	0.1936 (3)
O(3)	0.2768 (2)	−0.0739 (2)	0.3120 (2)	O(13)	0.4502 (5)	0.0540 (3)	0.0951 (4)
C(19)	0.4509 (3)	−0.0986 (3)	0.4166 (3)	C(37)	0.4567 (7)	0.3914 (5)	0.4230 (6)
C(20)	0.4624 (4)	−0.1183 (3)	0.3410 (4)	C(38)	0.3879 (8)	0.4274 (6)	0.3592 (7)
O(4)	0.4277 (3)	−0.0737 (2)	0.2807 (2)	N(6)	0.3276 (7)	0.4553 (6)	0.3066 (7)
N(2)	0.5076 (3)	−0.1814 (3)	0.3405 (3)	C(39)	0.2118 (8)	−0.3499 (7)	0.1175 (7)
C(21)	0.5209 (5)	−0.1976 (4)	0.2666 (4)	C(40)	0.1514 (12)	−0.3725 (10)	0.1511 (11)
C(22)	0.4526 (5)	−0.2523 (5)	0.2058 (4)	N(7)	0.1124 (11)	−0.3989 (10)	0.1797 (11)
C(23)	0.5444 (5)	−0.2419 (4)	0.4059 (4)				

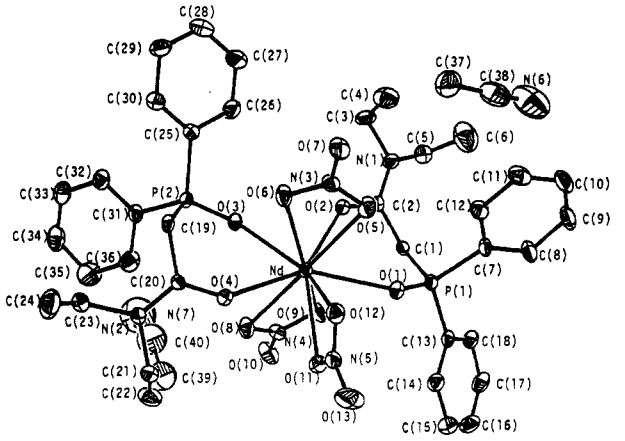

Figure 1. Molecular geometry and atom-labeling scheme for $Nd[Ph_2P(O)CH_2C(O)NEt_2]_2 \cdot 2MeCN$ (25% ellipsoids). Selected bond distances (Å): Nd–O(1), 2.459 (3); Nd–O(2), 2.497 (5); Nd–O(3), 2.454 (4); Nd–O(4), 2.488 (4); Nd–O(5), 2.678 (4); Nd–O(6), 2.585 (4); Nd–O(8), 2.699 (4); Nd–O(9), 2.592 (4); Nd–O(11), 2.532 (6); Nd–O(12), 2.534 (5); P(1)–O(1), 1.485, (4); P(1)–C(1), 1.810 (7); C(1)–C(2), 1.512 (8); C(2)–O(2), 1.260 (6).

of the monomeric unit, $Nd(NO_3)_3[Ph_2P(O)CH_2C(O)NEt_2]_2 \cdot 2MeCN$, which is designated as **3**, is shown in Figure 1. The Nd(III) ion is directly bonded to two bidentate, neutral (carbamoylmethyl)phosphine oxide ligands and three bidentate nitrate ions. The ten oxygen atoms from these ligands provide a coordination polyhedron which closely corresponds to that found in **4**.

Comparative structural data for related ten-coordinate Nd(III) complexes unfortunately are not available; however, the Nd–O(phosphoryl) distance, Nd–O(1) = 2.459 (3) Å and Nd–O(3) = 2.454 (4) Å, are predictably long compared to the distances in the eight-coordinate monodentate phosphine oxide complex $Nd[(BuS)C(O)CH_2C(O)CF_3]_3[Ph_3PO]_2$, 2.399 (10) and 2.423 (9) Å.[16] The Sm-O(phosphoryl) distance in ten-coordinate **4** is 2.418 (3) Å,[6] and it might appear that there is a lengthening of the Nd–O(phosphoryl) distance relative to the Sm–O(phosphoryl) distance. However, if the differences in ionic radii for the central metal atoms [1.09 Å for Sm(III), 1.12 Å for Nd(III)] are taken into account and a 3σ test is applied on the bond distance error estimates, it is concluded that the Nd–OP and Sm–OP bond distances are equivalent. This is not the anticipated result. If aryl groups on a phosphoryl functional group provide significantly increased electron density and donor strength to the phosphoryl oxygen atom in **1** it would be expected that the resulting Nd–O bond distance in **3** would be shorter.

The Nd–O(carbonyl) distances, Nd–O(2) = 2.497 (5) Å and Nd–O(4) = 2.488 (4) Å, in **3** are similar to those found in the eight-coordinate complex $Nd[(BuS)C(O)CH_2C(O)CF_3]_3$, 2.485 (8), 2.492 (10), and 2.501 (9) Å,[16] but long compared to the Nd–OC distance in $Nd[CH_3C(O)CH_2C(O)CH_3]_3 \cdot 2H_2O$, 2.44 (2) Å.[17] The Sm–O(carbonyl) distance in **4**, 2.433 (2) Å, appears to be slightly shorter than the comparable distance in **3** even after allowance is made for the difference in ionic radii.[18] Whether this trend results from steric or electronic factors is not clear at this time.

The coordination of the nitrate ions to Nd(III) appears to be normal. The NO_3^- ions are planar with Nd–O(nitrate)$_{av}$ = 2.60 ± 0.02 Å. This distance can be compared with the average distance in $Nd(Me_2SO)_4(NO_3)_3$, 2.64 (2) Å. The P–O(phosphoryl) distance in **3** is 1.485 (4) Å and the C–O(carbonyl)

(15) The nonbonded Nd···$NCCH_3$ separations in **3** are 6.73 and 7.52 Å. The closest nonbonded separation between a solvent molecule atom and an atom in the complex is C(39)···O(10), 3.13 Å.

(16) Leipoldt, J. G.; Bok, L. D. C.; Laubscher, A. E.; Basson, S. S. *J. Inorg. Nucl. Chem.* **1975**, *37*, 2477.

(17) Aslanov, L. A.; Porai-Koshits, M. A.; Dekaprilvich, M. O. *Zh. Strukt. Khim.* **1971**, *12*, 470.

(18) The average Nd–O(carbonyl) distance of 2.493 (5) Å can be compared with the ionic radii corrected Sm–O(carbonyl) distance of 2.463 (2) Å (2.433 + 0.03 Å). Application of a 3σ test in the distance error estimates results in the following distance ranges: Nd; 2.508, 2.479 Å Sm; 2.469, 2.457 Å. Clearly the greatest difficulty in assessing bond distance variations in these complexes involves the uncertainty introduced by the ionic radii correction. If it is assumed that the ionic radii have a deviation of ±0.01 Å then even the suggested difference in the M–OC bond distances disappears at the 3σ test level.

distance is 1.260 (6) Å. Unfortunately, structural parameters for the uncoordinated ligand are not available; however, the corresponding distances in $UO_2[Ph_2P(O)CH_2C(O)NEt_2](NO_3)_2$ are known: P–O = 1.512 (5) Å and C–O = 1.264 (8) Å. The slightly shorter P–O distance in **3** suggests that there is a smaller degree of electron transfer from the phosphoryl P–O bond to the Nd ion in **3**, which would be consistent with a weaker Nd–OP interaction.

At the level of accuracy of this structure determination no unusual structural features in the inner coordination sphere are revealed. In addition, no unusual intramolecular nonbonded distances or steric perturbations are found that could be responsible for the "aryl strengthening" effect. Apparently, factors that lead to the enhanced extraction ability of phenyl-substituted CMP ligands at high acid concentrations are not revealed in this solid-state structure analysis.

Acknowledgment. R.T.P. wishes to recognize the financial support for this research from the Department of Energy, Office of Basic Energy Sciences, Contract No. 82ER-10465.

Supplementary Material Available: Listings of structure factors, bond lengths, bond angles, anisotropic temperature factors, and hydrogen atom positional and thermal parameters (26 pages). Ordering information is given on any current masthead page.

Contribution from the Departamento de Química, Faculdade de Filosofia, Ciências e Letras de Ribeirão Preto, Universidade de São Paulo, 14.100 Ribeirão Preto, São Paulo, Brazil

Synthesis and Properties of the Ruthenium(II) Complexes *cis*-$Ru(NH_3)_4(isn)L^{2+}$. Spectra and Reduction Potentials

Luiz Alfredo Pavanin,[1a] Ernesto Giesbrecht,[1a] and Elia Tfouni*[1b]

Received September 25, 1984

In an earlier paper,[2] the synthesis and photochemical properties of trans-disubstituted tetraammineruthenium(II) complexes, *trans*-$Ru(NH_3)_4LL'^{2+}$ (where L and L' each are substituted pyridines) were reported. In order to extend the study we decided to examine the analogous cis system. Although the *cis*-dipyridyltetraammine complex *cis*-$Ru(NH_3)_4(py)_2^{2+}$ is known, examples of hetero bis-substituted complexes have not been previously isolated and characterized. However, rate[3,4] and cyclic voltammetry[5] studies indicate that the synthesis of the *cis*-tetraammineruthenium(II) complexes should be quite feasible. Described here are the synthesis and characterization of the *cis*-tetraammineruthenium(II) complexes *cis*-$Ru(NH_3)_4(isn)L^{2+}$, for which L = pyridine (py), 4-picoline (4-pic), isonicotinamide (isn), pyrazine (pz), or 4-acetylpyridine(4-acpy).

Experimental Section

Chemicals and Reagents. Ruthenium trichloride ($RuCl_3 \cdot 3H_2O$) (Strem) was the starting material for ruthenium complexes synthesis. Pyrazine (pz) (99.9%, Aldrich Gold Label) was used as supplied. Isonicotinamide (isn) (Aldrich) was recrystallized from water before use. 4-Picoline (4-pic) (Aldrich) and 4-acetylpyridine (4-acpy) were distilled before use. Sodium tetrafluoroborate ($NaBF_4$) was recrystallized from water. Ether, ethanol, and acetone were purified before use. Doubly distilled water was used throughout this work. All other chemicals were reagent grade and were used as supplied.

Ruthenium Complexes. *cis*-$[Ru(NH_3)_4(isn)Cl]Cl_2$ was prepared by following the literature procedure.[5]

cis-$[Ru(NH_3)_4(isn)L](BF_4)_2$ complexes were prepared by adapting the method described to prepare $[Ru(NH_3)_5L](BF_4)_2$[6] and *trans*-$[Ru(NH_3)_4LL'](BF_4)_2$.[2] A 100-mg (0.25-mmol) sample of *cis*-$[Ru(NH_3)_4(isn)Cl]Cl_2$ was dissolved in ~1.5 mL of water and deaerated with argon. Trifluoroacetic acid (TFA) (1 drop) and Zn(Hg) (~0.5 g) were then added, and the reaction was allowed to proceed for about 20 min with continuous argon bubbling. The resulting red solution was transferred under argon to a large excess of the ligand L. After 2 h of reaction time in the dark, the resulting solution was filtered and to it was added about 1 mL of a freshly prepared, deaerated, and almost saturated solution of $NaBF_4$ (~1 g/mL). After the mixture was cooled, the precipitate was collected by filtration, washed with ethanol and ether, and air-dried. The compounds were recrystallized several times in order to obtain analytically pure compounds. Recrystallizations were performed by dissolving the compounds in ~0.5–1.0 mL of warm deaerated water (~40 °C), filtering, and cooling in an ice bath. The precipitate was collected by filtration, washed, and dried as before. Prior to recrystallization, excess unreacted pyrazine in *cis*-$[Ru(NH_3)_4(isn)(pz)](BF_4)_2$ was eliminated by extraction with warm ethanol (~45 °C), which was done by suspending the crude compound in ethanol and then filtering.

Analysis. Carbon, hydrogen, and nitrogen microanalyses were performed by the staff of Dr. Riva M. Cruz of the Instituto de Química da Universidade de São Paulo.

Anal. Calcd for L = C_6H_7N: C, 25.8; N, 17.6; H, 4.5. Found: C, 25.8; N, 17.5; H, 4.3. Calcd for L = C_5H_5N: C, 24.3; N, 18.1; H, 4.3. Found: C, 24.6; N, 18.7; H, 4.2. Calcd for L = $C_6H_6N_2O$: C, 24.5; N, 19.1; H, 4.1. Found: C, 22.6; N, 18.8; H, 4.0. Calcd for L = C_7H_7NO: C, 26.6; N, 16.7; H, 4.3. Found: C, 27.2; N, 16.3; H, 4.3. Calcd for L = $C_4H_4N_2$: C, 22.0; N, 20.6; H, 4.1. Found: C, 22.4; N, 20.9; H, 4.2.

Cyclic Voltammetry. The cyclic voltammograms of the complexes were taken with a PARC electrochemical system consisting of a Model 175 universal programmer, a Model 173 potentiostat-galvanostat, and a RE 0074 X-Y Recorder, and with a CV-1B Cyclic Voltammograph from Bio-Analytical Systems and a Omnigraphic 100 X-Y Recorder from Houston Instrument. Scan rates of 20, 50, 100, 200, 300, 400, and 500 mV/s were employed. The electrochemical cells used were of the three-electrode type with Ag/AgCl in saturated potassium chloride solution as a reference electrode and platinum wire as an auxiliary electrode. The working electrode was a glassy-carbon electrode. All electrochemical data were obtained in supporting electrolyte solutions of 0.10 M ionic strength at 25 °C prepared from TFA and NaTFA at pH 3, and with millimolar concentrations of the complex. All solutions were deaerated with argon prior to the electrochemical measurements. The formal reduction potentials were calculated as the arithmetic mean of the anodic and cathodic peak potentials. E_f values were converted to NHE by adding 0.199 V.

Spectra. Electronic spectra were recorded at room temperature with a Beckman UV-5270 or a Varian 634-S recording spectrophotometer using quartz cells. Solutions used to measure extinction coefficients were prepared gravimetrically with quantitative dilution.

pK_a Determinations. A stock solution of the complex in water was used. The desired series of solutions with different acid (HCl) concentrations were obtained by dilution of measured volumes of the stock solutions of the complex and of HCl. The ionic strength (μ) was fixed at 1.0 M with sodium chloride. The pK_a values were determined by using the method described previously,[6,7] where log $(A_{\lambda_1}/A_{\lambda_2})$ is plotted against pH and λ_1 and λ_2 represent absorption maxima for the unprotonated (B) and protonated (BH^+) forms, respectively. The pK_a corresponds to the pH where log $(A_{\lambda_1}/A_{\lambda_2})$ equals log $(\epsilon(B)_{\lambda_1} + \epsilon(BH^+)_{\lambda_1})/(\epsilon(B)_{\lambda_2} + \epsilon(BH^+)_{\lambda_2})$. The reported p$K_a$ is average of three independent determinations.

Results and Discussion

Synthesis. The synthesis of the cis isomers of bis hetero-substituted ruthenium(II) tetraammines described here use the previously reported[5] *cis*-$[Ru(NH_3)_4(isn)Cl]Cl_2$ as the starting complex. From this point, the method used for the synthesis of ruthenium(II) pentaammines[6] was adapted for this case. In the synthetic paths were considered the stereoretentive substitution behavior of ruthenium(II) ammine-substitution reactions,[8] the

(1) (a) Instituto de Química da Universidade de São Paulo. (b) Departamento de Química da Faculdade de Filosofia, Ciências e Letras de Ribeirão Preto da Universidade de São Paulo.
(2) Tfouni, E.; Ford, P. C. *Inorg. Chem.* **1980**, *19*, 72.
(3) Allen, R. J.; Ford, P. C. *Inorg. Chem.* **1974**, *13*, 237.
(4) Isied, S. S.; Taube, H. *Inorg. Chem.* **1976**, *15*, 3070.
(5) Marchant, J. A.; Matsubara, T.; Ford, P. C. *Inorg. Chem.* **1977**, *16*, 2160.
(6) Ford, P. C.; Rudd, DeF. P.; Gaunder, R.; Taube, H. *J. Am. Chem. Soc.* **1968**, *90*, 1187.
(7) Clarke, R. E.; Ford, P. C. *Inorg. Chem.* **1970**, *9*, 495.

0020-1669/85/1324-4444$01.50/0